# Catalytic Cracking of Heavy Oil from Waste Plastic in Tapered Circulating Fluidized Bed Riser Reactor

*Parinya* Khongprom[1,*], *Thanapat* Whansungnoen[1], *Permsak* Pienduangsri[1], *Waritnan* Wanchan[1], and *Sunun* Limtrakul[2]

[1]Department of Industrial Chemistry, Faculty of Applied Science, King Mongkut's University of Technology North Bangkok, Bangkok, Thailand

[2]Department of Chemical Engineering, Faculty of Engineering, Kasetsart University, Bangkok, Thailand

**Abstract.** Because of the continuous increase in the amount of plastic waste, catalytic cracking is an interesting method that could be used to convert heavy oil from thermal cracking of plastic waste into fuel. The objective of this study was to investigate the hydrodynamic behavior and the performance of catalytic cracking of heavy oil in a circulating fluidized bed reactor using computational fluid dynamics. The two–fluid model incorporated with the kinetic theory of granular flow was applied to predict the hydrodynamic behavior with a reactive flow. Three reactor geometries were studied, which included a conventional riser, tapered–out riser, and tapered–in riser. The four–lump kinetic model was used to describe the catalytic cracking of heavy oil from waste plastic. A core–annulus flow pattern was found in the three reactor geometries. The solid fraction distribution of the tapered reactor was found to be more uniform than that of the conventional riser. The tapered–in riser showed the highest heavy oil conversion with the lowest gasoline selectivity. However, the heavy oil conversion and gasoline selectivity of the conventional and tapered–out reactors were not significantly different.

## 1 Introduction

The annual global production of plastic has been estimated to be 300 million tons and continuously increases annually [1, 2], resulting in large amounts of plastic waste being produced. The typical practical management of plastic waste involves landfills [3]. However, improper management may cause occupational health and environmental problems [4]. Additionally, the rapid growth of urbanization causes a lack of available land for landfills. Recently, pyrolysis has become an exciting technique that could convert plastic waste into fuel. Large polymer molecules have been thermally cracked to small molecular products, which mainly included heavy oil [5]. The heavy oil was further catalytic cracked to form more useful products, such as gasoline, kerosene, and diesel. The catalytic cracking reaction involves a fast reaction with a complex kinetic mechanism. Several lump kinetic models have been proposed to describe the progress of the chemical reaction in systems based on the catalyst used and the type of heavy oil [6-8].

Circulating fluidized bed (CFB) riser reactors offer a high potential to carry on such a gas–solid reactive flow with a high reaction rate. CFB risers are broadly applied to operate numerous chemical reactions, such as the $CO_2$ sorption reaction [9], catalytic cracking reaction [10], and coal combustion [11]. Thus, numerous researchers have attempted to explore the detailed flow behavior of this type of reactor. One of the crucial factors influencing the hydrodynamics is the reactor geometry. In a conventional riser with a constant diameter, the core–annulus flow structure, which is a uniform distribution in the core region and has a high solid fraction in the near–wall region, has been reported [12, 13]. However, the radial flow behavior in the tapered–out riser is more uniform. The core–annulus flow pattern has been shown to disappear in a well–designed tapered–out riser [14]. The decrease in the riser diameter enhances the turbulence and mixing in the system [15]. The tapered–in riser exhibits a high solid residence time with a uniform temperature distribution [15]. Chalermsinsuwan *et al*. [16] studied the performance of the propane combustion reaction in different riser geometries. The tapered–out riser is suitable for operating fast reactions. Meanwhile, slow reactions should be performed in the tapered–in riser. However, a study of the catalytic cracking of heavy oil in various reactor geometries is rare in the literature owing to the complex mechanism of the multiple reactions.

Currently, the computational fluid dynamics (CFD) method offers many advantages for studying the flow behavior in a multiphase system. The useful model for gas–solid flow system with a high solid content is the two–fluid model coupled with the kinetic theory of granular flow. A numerical method associated with a mathematical model related to the two-fluid model has been developed to ensure accurate and realistic simulation results [17-18]. The model parameter

* Corresponding author: parinya.k@sci.kmutnb.ac.th

sensitivity has been systematically studied to explore the appropriate guidelines for practical application of the model [13, 19]. This model was further developed to study reactive flow fluidized beds. Lan *et al*. [20] studied the catalytic cracking of petroleum fractions using a CFD simulation. The simulation results were validated with experimental data on the lab-scale and industrial-scale reactors. The predicted hydrodynamics and chemical performance reasonably agreed with experimental data. This study aimed to apply a CFD model to investigate the hydrodynamic behavior and the performance of the catalytic cracking in various riser geometries.

## 2 Simulation method

### 2.1 Reactor geometry

Three CFB riser geometries were investigated in this study as shown in Fig. 1, which are the conventional (1a), tapered–in (1b), and tapered–out (1c) configurations. The volume and height of all reactors were kept constant at 0.446 $m^3$ and 14.2 m, respectively. The conventional riser has a constant reactor diameter of 0.2 m. The inlet and outlet diameters of the tapered–in riser are 0.1255 and 0.274 m, respectively. Inversely, the inlet and the outlet diameters of the tapered–out riser are 0.274 and 0.1255 m, respectively. A two dimensional flow domain was considered in this study owing to the low computational cost with acceptable simulation results [15].

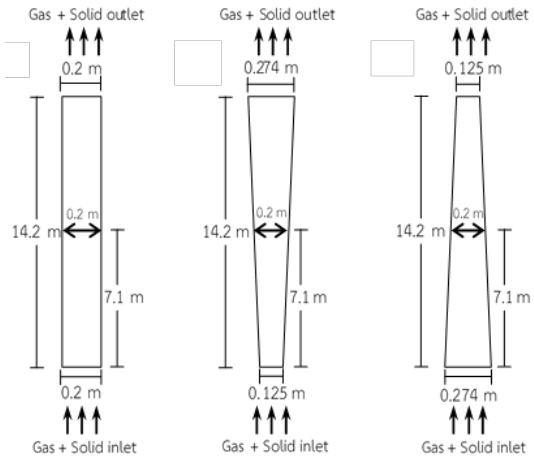


**Fig. 1.** Reactor geometries used in this study: conventional riser (a), tapered–in riser (b), tapered–out riser (c).

### 2.2 Kinetics of catalytic cracking

Catalytic cracking of high molecular weight hydrocarbon yields a mixture of individual lower molecular weight products. The individual product species were classified into a small group or lump according to their boiling point. This lumping technique was useful for kinetic study of this type of system. The number of lump, the kinetic scheme and the kinetic rate constant depend on several factors, such as the type of feedstock and catalyst used. The four lump kinetic model of the catalytic cracking of heavy oil from waste plastic, which was proposed by Songip *et al*. [7], was used in this study. This model included heavy oil (A), gasoline (B), light gas (C) and coke (D). The cracking mechanism is shown in Fig. 2. Heavy oil was cracked to gasoline, light gas, and coke. Gasoline can be further cracked to light gas and coke. The kinetic rate constants were used from Songip *et al*. [7].

### 2.3 Mathematical model

The two–fluid model coupled with the kinetic theory of granular flow was used to simulate the hydrodynamic behavior and performance of the chemical reaction. The k–ε turbulent model was used to describe the turbulence of gas and solid phases. The governing equations are as follows.

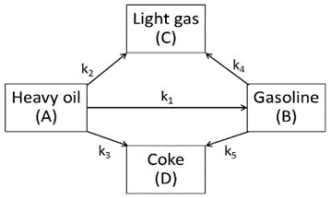


**Fig. 2.** 4–lumps kinetic model.

Continuity equation

Gas phase:

$$\frac{\partial}{\partial t}(\alpha_g \rho_g) + \nabla \cdot (\alpha_g \rho_g \vec{v}_g) = 0 \tag{1}$$

Solid phase:

$$\frac{\partial}{\partial t}(\alpha_s \rho_s) + \nabla \cdot (\alpha_s \rho_s \vec{v}_s) = 0 \tag{2}$$

Momentum equation

Gas phase:

$$\frac{\partial}{\partial t}(\alpha_g \rho_g \vec{v}_g) + \nabla \cdot (\alpha_g \rho_g \vec{v}_g^2) = -\alpha_g \cdot \nabla p + \nabla \cdot \overline{\overline{\tau}}_g + \alpha_g \rho_g \vec{g} + K_{gs}(\vec{v}_g - \vec{v}_s) \tag{3}$$

Solid phase:

$$\frac{\partial}{\partial t}(\alpha_s \rho_s \vec{v}_s) + \nabla \cdot (\alpha_s \rho_s \vec{v}_s^2) = -\alpha_s \cdot \nabla p - \nabla \cdot p_s + \nabla \cdot \overline{\overline{\tau}}_s + \alpha_s \rho_s \vec{g} + K_{gs}\left(\vec{v}_s - \vec{v}_g\right) \tag{4}$$

Granular temperature

$$\frac{3}{2}\left[\frac{\partial}{\partial t}(\alpha_s \rho_s \Theta_s) + \nabla \cdot (\alpha_s \rho_s \vec{v}_s \Theta_s)\right] = \left(-P_s \overline{\overline{I}} + \overline{\overline{\tau}}_s\right) : \nabla \vec{v}_s + \nabla \cdot (k_{\Theta s} \nabla \Theta_s) - \gamma_{\Theta s} \tag{5}$$

Species conservation equation

$$\frac{\partial}{\partial \mathrm{t}}(\alpha_g \rho_g C_{g,i}) + \nabla \cdot (\alpha_g \rho_g v_g C_{g,i}) = \nabla \cdot \left(\alpha_g \Gamma_i \nabla C_{g,i}\right) + r_i' \quad (6)$$

k–ε turbulence model

Turbulence kinetic energy:

$$\frac{\partial}{\partial t}(\alpha_j \rho_j k_j) + \nabla \cdot (\alpha_j \rho_j k_j U_j) = \nabla \cdot \left( \varepsilon_j \frac{\mu_t}{\sigma_k} \nabla k_j \right) + (\alpha_j G_k - {}_j \rho_j \varepsilon_j) \quad (7)$$

Dissipation rate equation of turbulence energy:

$$\frac{\partial}{\partial t}(\alpha_j \rho_j \varepsilon_j) + \nabla \cdot \left(\alpha_g \rho_g \varepsilon_j U_j\right) = \nabla \cdot \left( \varepsilon_j \frac{\mu_t}{\sigma_k} \nabla \varepsilon_j \right) + \frac{\varepsilon_j}{k}\left(C_{1\varepsilon} \alpha_j G_k - C_{2\varepsilon} \alpha_j \rho_j \varepsilon_j\right) \quad (8)$$

A commercial CFD package, Ansys–Fluent, was employed to perform the simulation. The finite volume method was adopted to solve the governing equations. The SIMPLE algorithm was used to solve for the pressure–velocity correction. The inlet mass flow rates of gas and solid particles, which were 0.92 and 53.30 kg/s, respectively, were kept constant. The boundary conditions and the model parameters are listed in Table 1.

**Table 1.** Boundary conditions and model parameters used in this study.

| Boundary condition/ Parameter | Value/Type |
|---|---|
| Boundary conditions: | |
| Wall | |
| - Gas | No slip |
| - Particle | Partial slip |
| Inlet | Velocity-inlet |
| Outlet | Pressure-outlet |
| Parameter: | |
| Particle diameter ($d_s$) | 75 μm |
| Particle density ($\rho_s$) | 1500 kg/m$^3$ |
| Restitution coefficient of particle-particle ($e_s$) | 0.95 |
| Restitution coefficient of particle-wall ($e_w$) | 0.9 |
| Specularity coefficient (Φ) | 0.5 |
| Inlet granular temperature (Θ) | 0.0001 m$^2$/s |

## 3 Results and discussion

### 3.1 Model validation

The hydrodynamic behavior and the chemical performance of the conventional riser were used to validate the simulation results. The simulated hydrodynamics were first validated by comparing with the experimental results from Knowlton [21] in terms of the radial distribution of the voidage, as shown in Fig. 3. Acceptable quantitative agreement with the experimental data was obtained.

The distribution of the heavy oil mass fraction was used to validate the chemical performance of these simulation results with those of the ideal reactors, which were ideal plug flow and ideal mixed flow reactors. Fig. 4 displayed the heavy oil mass fraction under various time factors. The heavy oil mass fraction decreased with an increase in the time factor. The performance of the riser reactor is closer to that of the ideal plug flow than that of the ideal mixed flow. The plug flow behavior was approached in the center region owing to the uniform flow pattern. However, the particle cluster near the wall caused high back–mixing in this region. Therefore, the performance of the riser reactor slightly deviated from the ideal plug flow reactor.

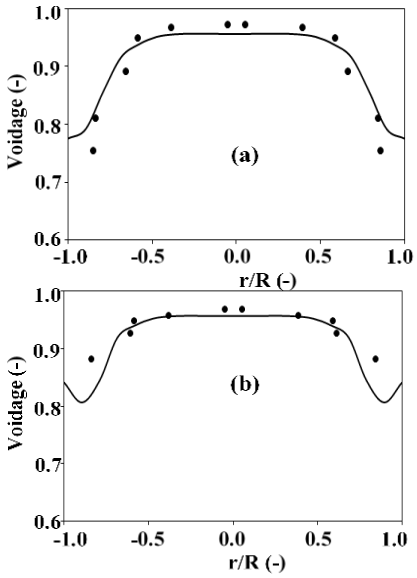


**Fig. 3.** Comparison of the voidage radial profile with the experimental data from Knowlton [21] (marker): (a) at 3.9 m. height, (b) 8.1 m. height.

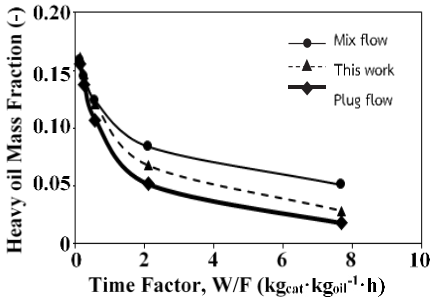


**Fig. 4.** Comparison of the heavy oil mass fraction obtained from this study with those from the ideal reactors.

### 3.2 Effect of reactor geometry on the hydrodynamic behavior

Hydrodynamic behavior is not only the key to design and operation but also influences the chemical performance. The effect of the reactor geometry on the radial and axial directions of the solid volume fraction and the gas and solid velocities was discussed in this

section. It was found that the reactor geometry considerably affected the flow behavior. Fig. 5 showed the radial distribution of the solid volume fraction for various reactor geometries. At z = 2 m, different profiles were observed. In the conventional riser, the solid fraction was uniform and slightly increases toward the wall. The fraction was uniform in the center and considerably increases near the wall of the tapered–out riser. A large particle cluster was formed near the wall of the tapered–in riser because high Gs and Ug were fed into the reactor. At higher reactor heights, all risers exhibited a core–annulus flow pattern. The core region of the tapered–out riser was the largest with 0<r/R<0.8. In contrast, the core region of the tapered–in riser was the smallest with 0<r/R<0.55.

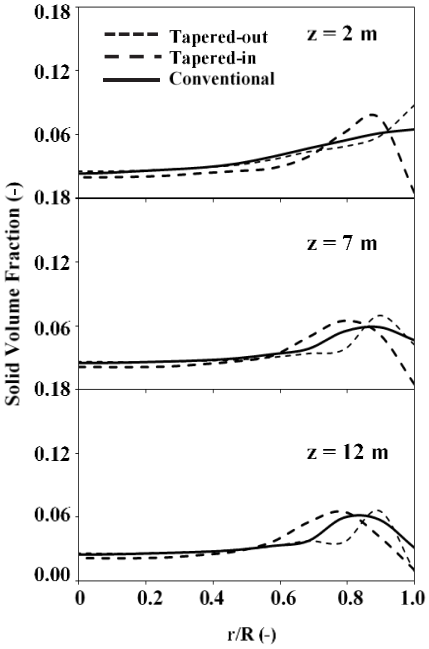


**Fig. 5.** Radial distribution of solid volume fraction for various axial positions.

Fig. 6 displayed the axial profile of the solid volume fraction for different riser reactors. In the tapered–in riser, the solid fraction significantly decreased near the inlet and rapidly approached a constant value within a short distance from the inlet. The solid fraction of the tapered–in riser was lower than that of the conventional riser. However, the solid fraction in the tapered–in riser was considerably higher than that of the conventional riser, as reported by Chalermsinsuwan *et al*. [15]. The same Ug was used in their study, resulting in a very low gas mass flow rate in the tapered–in riser. In the tapered–out riser, the fraction decreased along the reactor height because of the continuous decreased in the riser diameter. Additionally, the solid fraction of the tapered–out riser and the conventional riser were almost the same. However, Chalermsinsuwan *et al*. [15] found that the solid fraction of the tapered-out riser was significantly lower than that of the conventional riser owing to the higher mass flow rate of gas in the tapered–out riser.

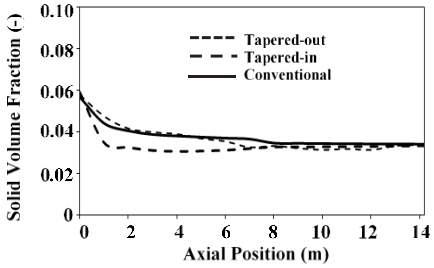


**Fig. 6.** Axial distribution of solid volume fraction for different riser geometries.

Fig. 7 showed the radial profile of gas and solid velocities. At z = 2 m, gas and solid velocities slowly decreased in the lateral direction for all riser types. However, the gas and solid velocities of the tapered–in riser are high with slight increases near the wall because of the high inlet gas velocity. A more uniform distribution occured with the increased height of the reactor. At z = 7 m, the riser geometry insignificantly affected the gas and solid velocities. At z = 12 m, the gas and solid velocities of the tapered–out riser were high because the smallest riser reactor was in the axial position. Fig. 8 showed the axial distributions of the gas and solid velocities. In the inlet region, a large velocity difference was observed for all riser geometries. A high gas velocity significantly caused the particle to move upward resulting in a rapid increase in the solid velocity and a considerable decrease in the gas velocity. In the fully developed flow region of a conventional riser, gas and solid velocities are constant and almost the same. No fully developed flow regions were observed in the tapered risers. Above the inlet region of the tapered–out riser, the gas and solid velocities continuously increased along the reactor height due to the decreasing riser reactor diameter. Inversely, the gas and solid velocities slowly decreased along the reactor height of the tapered–in riser.

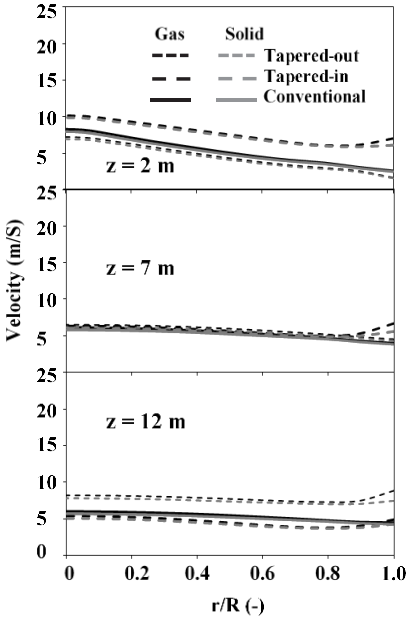


**Fig. 7.** Radial distributions of solid gas and solid velocities for various axial positions.

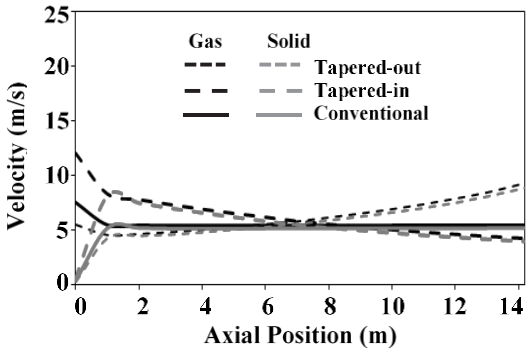


**Fig. 8.** Axial distributions of gas and solid velocities for different riser geometries.

### 3.3 Effect of reactor geometry on the catalytic cracking reaction

The chemical performance of catalytic cracking with various reactor geometries was investigated. The heavy oil mass fraction, gasoline mass fraction, heavy oil conversion and gasoline selectivity were chosen for indicating the chemical performance. The effect of riser geometry on the radial distribution of the heavy oil mass fraction was shown in Fig. 9. An almost uniform distribution was observed, indicating the plug flow behavior in the system. At 2 m, however, the heavy oil mass fraction slightly decreased toward the wall. A high heavy oil mass fraction was obtained in the tapered–in riser. Fig. 10 showed the radial distribution of the gasoline mass fraction, which is the desired product. An almost uniform distribution was also observed. The gasoline mass fraction of the tapered–in riser was considerably lower than those from the conventional and tapered–out risers.

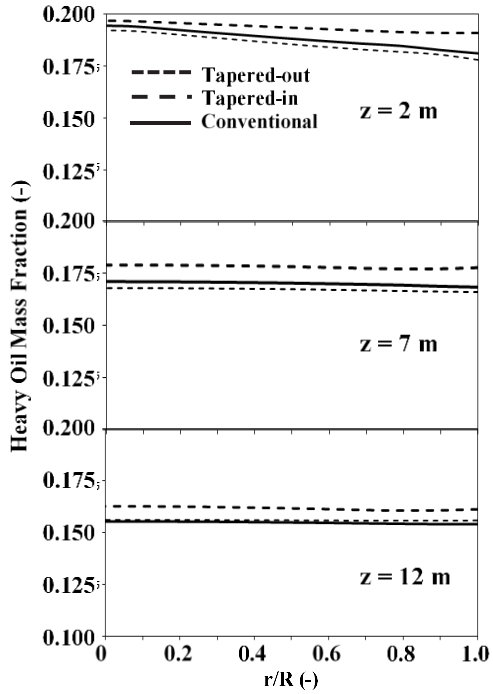


**Fig. 9.** Radial distributions of heavy oil mass fraction for various axial positions.

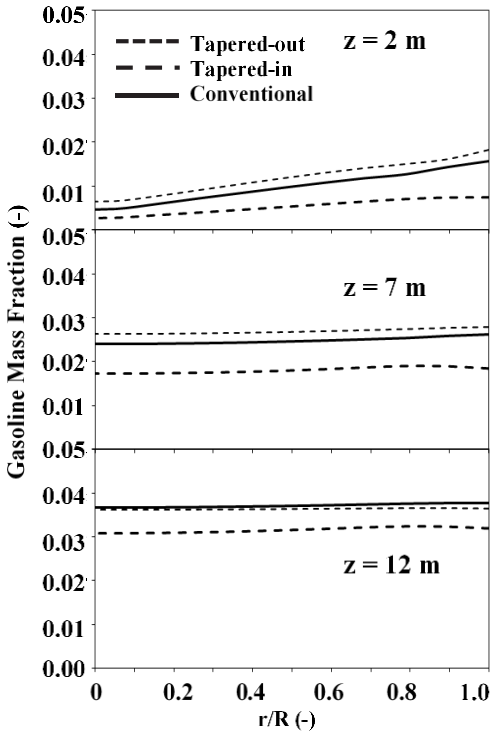


**Fig. 10.** Radial distributions of gasoline mass fraction for various axial positions.

The axial distribution of the heavy oil conversion was shown in Fig. 11. The conversion tended to increase along the height as the reaction progresses. Near the inlet section, the conversion of the tapered–out riser rapidly increased, indicating a high reaction rate. This was because the inlet gas velocity was very low (see Fig. 8) and there was a high solid volume fraction (see Fig. 6). In the outlet region, however, the conversion of the tapered–out riser was lower than that of the conventional riser because of the high gas velocity and low solid fraction. In addition, the conversion of the tapered–in riser was the lowest owing to the low solid fraction especially in the lower section of the reactor.

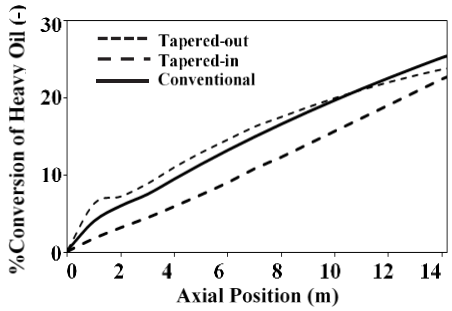


**Fig. 11.** Axial distribution of heavy oil conversion for different riser geometries.

Fig. 12 displayed the axial profile of the gasoline selectivity. Although the heavy oil conversion was lowest in the tapered–in riser, the gasoline selectivity was the highest. In the tapered–out riser, the gasoline selectivity was the lowest, indicating the over cracking of gasoline.

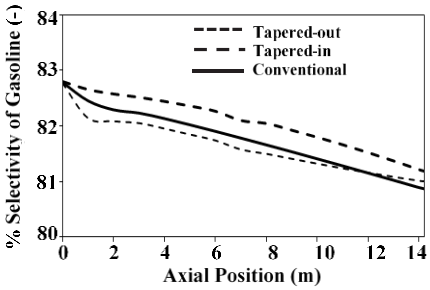


**Fig. 12.** Axial distribution of gasoline selectivity for different riser geometries.

## 4 Conclusions

The hydrodynamics and the chemical performance of the catalytic cracking of heavy oil for different riser geometries were studied via a CFD simulation. The core–annulus flow pattern was observed for all riser geometries. A large core area with a small particle cluster near the wall region was obtained in the tapered–out riser. There were no fully developed flow regions in the tapered riser. The tapered–in riser exhibited the lowest conversion of heavy oil and a higher gasoline selectivity. The tapered–out riser produced the highest heavy oil conversion and the lowest gasoline selectivity. Near the outlet region, however, the conversion of the tapered–out riser was lower than that of the conventional riser owing to the very high gas and solid velocities.

## Notation

| | |
|---|---|
| $C_D$ | drag coefficient |
| $C_{1\varepsilon}$, $C_{2\varepsilon}$ | turbulence constant |
| $d_p$ | particle diameter |
| $\vec{g}$ | gravitational acceleration, m s$^{-2}$ |
| $G_s$ | solid circulation rate, kg m$^{-2}$s$^{-1}$ |
| $\overline{\overline{I}}$ | unit tensor |
| $k_j$ | turbulent kinetic energy, J kg−1 |
| $k_\Theta$ | diffusion granular temperature coefficient, kg m$^{-1}$ s$^{-1}$ |
| P | pressure, kPa |
| U | superficial gas velocity, m s$^{-1}$ |
| $\vec{v}$ | velocity, m s$^{-1}$ |
| Greek symbol | |
| $\varepsilon$ | turbulent dissipation rate, m$^2$ s$^{-3}$ |
| $\alpha$ | volume fraction |
| $\mu$ | viscosity, kg m$^{-1}$s$^{-1}$ |
| $\rho$ | density, kg m$^{-3}$ |
| $\overline{\overline{\tau}}$ | stress tensor, Pa |
| $\Theta$ | granular temperature, m$^2$ s$^{-2}$ |
| $\emptyset$ | energy exchange between phases, kg m$^{-1}$s$^{-2}$ |
| $\Gamma_i$ | energy dissipation, kg m$^{-1}$s$^{-2}$ |
| Subscript | |
| $g$ | gas phase |
| $s$ | solid phase |

This research was funded by Faculty of Applied Science, King Mongkut's University of Technology North Bangkok, Contract no. 6241105.

## References

1. R. Miandad, M.A. Barakat, A.S. Aburiaziaza, M. Rehan, A.S. Nizami, Proc Safety Environ Protect. **102**, 822-838 (2016)
2. D. K. Ratnasari, M. A. Nahil, P.T. Williams, J. Anal. Appl. Pyrolysis, **124**, 631-637 (2017)
3. I. M. Gandidi, M. D. Susila, A. Mustofa, N. A. Pambudi, J Energy Inst. **91**, 304-310 (2018)
4. L. C. Alexandra, *Municipal solid waste: Turning a problem into resource, Waste: The challenges facing developing countries* (Urban Specialist, World Bank, 2012)
5. M. Rehan, R. Miandad, M. A. Barakat, I. M. I. Ismail, T. Almeelbi, J. Gardy, Int Biodeterior Biodegrad. **119**, 162-175 (2017)
6. L.-S. Lee, Y.-W. Chen, T.-N. Huang, Can Chem Eng J. **67**, 615-619 (1989)
7. A. R. Songip, T. Masuda, H. Kuwahara, K. Hashimoto, Energy & Fuels, **8**, 131-135 (1994)
8. X. Lan, C. Xu, G. Wang, L. Wu, J. Gao, Chem Eng Sci. **64**, 3847-3858 (2009)
9. P. Khongprom, D. Gidaspow, Particuology, **8**, 513-535 (2010)
10. J. Gao, C. Xu, S. Lin, G. Yang, Y. Guo, AIChE J. **47**, 677-692 (2001)
11. S. Wang, J. Chen, G. Liu, H. Lu, F. Zhao, Y. Zhang, Fuel Process Technol., **126**, 163–172 (2014)
12. C. Chen, J. Werther, S. Heinrich, H. Y. Qi, E. U. Hartge, Powder Technol., **235**, 238-247 (2013)
13. A. Almuttahar, F. Taghipour, Powder Technol., **185**, 11-23 (2008)
14. L. Huilin, Z. Yunhua, S. Zhiheng, J. Ding, J. Jiying, Powder Technol., **169**, 89-98 (2006)
15. B. Chalermsinsuwan, P. Kuchonthara, P. Piumsomboon, Chem Eng Process, **48**, 165-177 (2009)
16. B. Chalermsinsuwan, P. Kuchonthara, P. Piumsomboon, Chem Eng Process, **49**, 1144-1160 (2010)
17. D. Gidaspow, *Multiphase flow and fluidization: Continuun and kinetic theory description* (Academic Press, Boston, 1994)
18. M. Syamlal, T. O. Brien, *Derivation of drag coefficient from velocity-voidage correlation* (U.S. Dept. of Energy, Office of Fossil Energy, West Virginia, 1987)
19. M. T. Shah, R. P. Utikar, M. O. Tade, V. K. Pareek, Chem Eng J. **168**, 812-821 (2011)
20. X. Lan, C. Xu, G. Wang, L. Wu, J. Gao, Chem Eng Sci. **64**, 3847-3858 (2009)
21. T. Knowlton, D. Geldart, J. Matsen, D. King, *(Eighth International Fluidization Conference, France, 1995)*